Transport, Magnetic and Vibrational Properties of Chemically Exfoliated Few Layer Graphene

Bence G. Márkus[1], Ferenc Simon[*,1], Julio C. Chacón-Torres[2], Stephanie Reich[2], Péter Szirmai[3], László Forró[3], Thomas Pichler[4], Philipp Vecera[5], Frank Hauke[5], Andreas Hirsch[5]

[1] Department of Physics, Budapest University of Technology and Economics, POBox 91, Budapest, H-1521, Hungary
[2] Institute of Experimental Physics, Free University Berlin, Arnimallee 14., Berlin, 14195, Germany
[3] Institute of Physics of Complex Matter, FBS Swiss Federal Institute of Technology (EPFL), CH-1015 Lausanne, Switzerland
[4] Faculty of Physics, University of Vienna, Strudlhofgasse 4., Vienna, A-1090, Austria
[5] Department of Chemistry and Pharmacy and Institute of Advanced Materials and Processes (ZMP), University of Erlangen-Nuremberg, Henkestrasse 42., Erlangen, 91054, Germany

Received XXXX, revised XXXX, accepted XXXX
Published online XXXX

Key words: Graphene, chemical exfoliation, Raman, ESR, microwave conductivity.

[*] Corresponding author: e-mail f.simon@eik.bme.hu, Phone: +36-1-463-1215, Fax: +36-1-463-4180

We study the vibrational, magnetic and transport properties of Few Layer Graphene (FLG) using Raman and electron spin resonance spectroscopy and microwave conductivity measurements. FLG samples are produced using wet chemical exfoliation with different post processing, namely ultrasound treatment, shear mixing, and magnetic stirring. Raman spectroscopy shows a low intensity D mode which attests a high sample quality. G mode is present at 1580 cm^{-1} as expected for graphene. The 2D mode consists of 2 components with varying intensities among the different samples. This is assigned to the presence of single and few layer graphene in the samples. ESR spectroscopy shows a main line in all types of materials with a width of about 1 mT and and a g-factor in the range of $2.005 - 2.010$. Paramagnetic defect centers with a uniaxial g-factor anisotropy are identified, which shows that these are related to the local sp^2 bonds of the material. All kinds of investigated FLGs have a temperature dependent resistance which is compatible with a small gap semiconductor. The difference in resistance is related to the different grain size of the samples.

1 Introduction Novel carbon allotropes gave an enormous boost to condensed-matter and molecular physics at the end of the last century. The process was started with the discovery of fullerenes [1] and carbon nanotubes [2], but for the biggest breakthrough we had to wait until 2004 [3]. Graphene since its discovery become one of the most important materials in condensed-matter physics. Being the basis of all other novel carbon allotropes [4,5] (fullerenes, nanotubes, graphite) understanding graphene is crucial. Interesting physical such as mechanical (e.g. high fracture strength, high elasticity) and electronic properties (e.g. low resistance, high carrier mobility, quantum Hall-effect) prospects useful applications of these novel carbon materials [6]. However, one of the remaining obstacles for the applicability of graphene is mass production with controlled quality and graphene layer size.

High quality material can be prepared with mechanical exfoliation (also referred as mechanical cleavage) can be prepared but only in small amounts (maximum available is still in the scale of microns [7]) on various substrates. Epitaxial growth of graphene on various substrates [8–10] is an alternative but the up-scalability of this method is limited and the resulting sample qualities needs yet to be improved. On the other hand, with chemical vapor deposition (CVD) high yields are achievable [11–17] in a poorer quality due to the enormous number of defects. An other problem with the CVD method that it still requires a substrate. Being a material of an atomic thin layer on a substrate is a

serious issue when one would like to apply bulk characterization methods such as Electron Spin Resonance Spectroscopy (ESR) or macroscopic transport measurements (e.g. microwave conductivity). The substrate also has a negative effect on the electronic and vibrational properties of graphene (e.g. electronic interactions, various strains apply). These effects are visible when one tries to compare the results of free standing graphene [18] with graphene on other substrates: [19] (Si-SiO_2), [20] (Si-SiO_2 and ITO), [21] (SiC), [22] (glass).

Other ways to create graphene in a mass production is reduction from graphite/graphene oxide (GO) and wet chemical exfoliation from graphite intercalation compounds (GICs) with various solvents. Reduction process is feasible in many chemical and biological routes with different quality of the final product [23–35]. In general, the quality of final product may vary in a large scale but always contains residual oxygen, missing carbon atoms, free radicals, and dangling bonds therefore one can end up with a thermally metastable material.

Wet chemical or liquid phase exfoliation is the most promising way to mass produce high quality materials without disturbing the effects of the substrate [36–41]. For the optimal quality of the outcome the effect of solvent [42] and the mechanical post procession has to be examined. Here we report the transport, magnetic and vibrational properties of Wet Chemically Exfoliated (WCEG) Few Layer Graphene (FLG) using microwave conductivity, electron spin resonance and Raman spectroscopies.

2 Experimental We studied three WCEG species which were prepared by different mechanical routes: ultrasounded (US), shear mixed (SM) and stirred (ST). All kinds were produced from saturate intercalated potassium graphite powder, KC_8 using DMSO solvent for wet exfoliation (full protocol described in Ref. [42]). The starting material, SGN18 graphite powder (Future Carbon) and Grade I bulk HOPG (SPI) were taken into comparison. Mechanical post processing were ultrasound treatment, shear mixing and magnetic stirring. The procedure was done under argon atmosphere. The pristine materials were cleaned under high vacuum (10^{-7} mbar) at $400°$C for one hour to get rid of the remaining solvent and impurities. Raman measurements were carried out in a high sensitivity single monochromator LabRam spectrometer [43] using 514 nm laser excitation, $50\times$ objective with 0.5 mW laser power. For ESR measurements a Bruker Elexsys E580 X-band spectrometer was used. Microwave conductivity measurements were done with the cavity perturbation technique [44,45] extended with an AFC feedback loop to increase precision [46]. The photographs were taken with a Nikon Eclipse LV150N optical microscope using $5\times$ (for FLG) and $10\times$ (for SGN18) objectives.

3 Results and Discussion To get an insight which mechanical post production method produces the best quality the vibrational, electronic and transport properties of the materials have to be investigated. We discuss the Raman, ESR and microwave conductivity results.

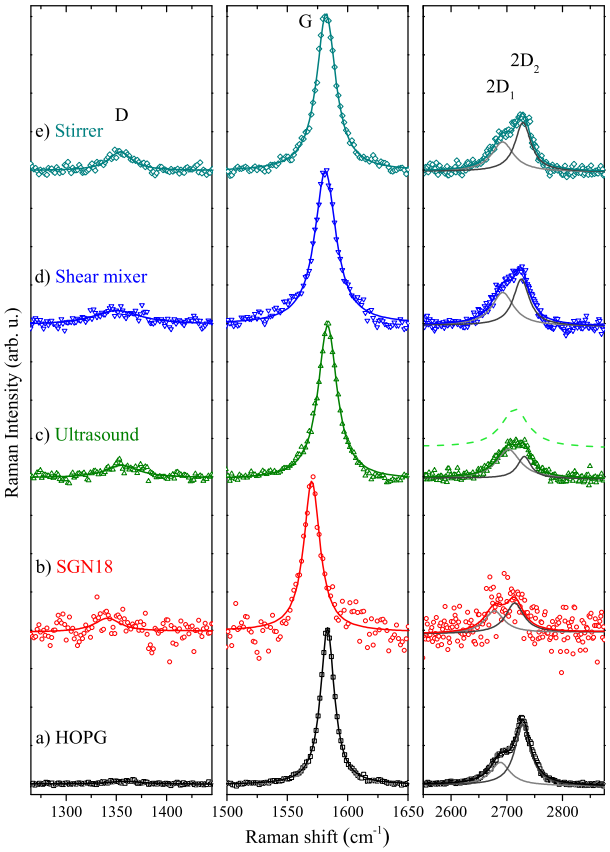

Figure 1 D, G, 2D Raman modes of the investigated species using 514 nm laser excitation. a) bulk HOPG, b) SGN18 graphite powder, c) ultrasound sonicated exfoliated graphene, d) shear mixed exfoliated graphene, e) stirred exfoliated graphene. Solid color line represents Lorentzian-fits, grey lines denotes the decomposition of the 2D peaks. The dashed green line in case of the ultrasound sample points that the 2D peak can be fitted with one single Lorentzian as well.

3.1 Raman spectroscopy Raman spectra of the examined samples are shown in Fig. 1. Namely, the D, G, and 2D Raman modes are shown. Solid lines represent Lorentzian fits. In most cases 2D lines are made up of 2 components, namely $2D_1$ and $2D_2$. In the case of ultrasound preparation the 2D feature can also be well fitted with one single Lorentzian. Parameters of the fitted Lorentzian curves are given in Table 3.1.

Several observations can be made from the data in Table 3.1. one can make the following conclusions. The Raman spectrum properties of graphite powder differs from HOPG. This is not an instrumental artifact, position and

width of peaks in case of graphite strongly depends on morphology and grain size [47].

Table 1 Parameters of the fitted Lorentzian curves for the D, G, and 2D Raman modes for a 514 nm excitation. ν denotes the position and $\Delta\nu$ the FWHM in cm^{-1}, * stands for single Lorentzian fit.

514 nm	HOPG	SGN18	US	SM	ST
ν_D	1358.4	1341.1	1355.5	1350.6	1353.9
$\Delta\nu_D$	18.6	15.5	20.0	29.4	14.2
ν_G	1583.3	1570.3	1583.3	1581.6	1582.2
$\Delta\nu_G$	6.9	8.1	9.5	10.6	9.6
ν_{2D_1}	2688.4	2677.5	2702.9	2692.8	2692.4
$\Delta\nu_{2D_1}$	21.4	21.4	25.7	23.7	23.9
ν_{2D_2}	2728.6	2714.1	2731.3	2726.1	2729.0
$\Delta\nu_{2D_2}$	17.1	19.6	14.7	17.4	17.3
ν^*_{2D}			2714.6		
$\Delta\nu^*_{2D}$			29.4		

The D peak is less pronounced when ultrasound sonication or shear mixing was applied in case of exfoliated graphenes. The position of the D peak varies between the graphite powder and HOPG. According to mechanically exfoliated and CVD studies [19,12] the D peak is expected at about 1350 cm^{-1} which is in a good agreement with our results. Both Ferrari and Das [20] agrees that the intensity of the D peak for single layer material has to be small. The ultrasounded and shear mixed material satisfies this criterion. The D peak is always present in wet chemically exfoliated graphenes [38,39] but its intensity is flake-size dependent [40]. The wet exfoliation according to the D peak intensity is far better in quality than for reduced GO samples [23,25,30].

All our FLG samples have a sharp G peak very close to HOPG (we remind that the starting material is SGN18). The width is about ~ 2 cm^{-1} broader than graphite (both powder and bulk). Position of the G mode varies around 1580 cm^{-1} in good agreement with previous studies [19, 20]. The G position also depends on the substrate and the number of layers. According to Ref. [18], the G peak position for the shear mixed and ultrasounded materials are very close to free standing graphene.

The 2D peak for single layer graphene is expected to be a single, symmetric peak [19]. The position of the peak is about 2700 cm^{-1} and shows a variation in the literature [19,20,36,37]. Width of the peak also varies in a wide scale from 15 up to 40 cm^{-1}. Variations can be explained with the effect of the substrate (samples on substrates always present a narrower peak) and the effect of preparations (strain, compressive forces may apply, chemicals may remain). Our FLG samples show two components for the 2D line. The position of the lower $2D_1$ peak agrees with previous single layer studies, thus this component is associated with single layer graphene sheets. The $2D_2$ peak position is close to that of graphite. The presence of the $2D_2$ mode can be interpreted as the presence of few layer sheets up to 4 layers. The width of the peaks suggest that we are dealing with single and few layer graphenes unlike in turbostratic graphite (in that case the width of 2D would be about 50 cm^{-1} [19]). Bilayer graphene has a unique 2D peak made up of 4 components [19], which is not present here. In case of the ultrasounded sample, the 2D peak can also be well fitted with one single Lorentzian with a position up to 2715 cm^{-1}.

The intensity (amplitude) ratios of 2D and G peaks are given in Table 3.1.

Table 2 Intensity (amplitude) ratios of 2D and G peaks, * notes the single Lorentzian fit.

514 nm	HOPG	SGN18	US	SM	ST
I_{2D_1}/I_G	0.21	0.17	0.21	0.27	0.37
I_{2D_2}/I_G	0.42	0.22	0.22	0.36	0.25
I_{2D}/I_G	0.63	0.39	0.43	0.63	0.62
I^*_{2D}/I_G			0.24		

Previous studies suggest that the number of layers can be extracted from this ratio [20,48,22]. Several other effect, including e.g. the effect of substrate (coupling-effect), the strain or compression, the method of the preparation, the type and quality of the solvent and the wavelength of laser excitation also affects the 2D to G Raman signal ratio. Therefore the ratio of I_{2D}/I_G has to be treated with care. The ratio in case of mechanically exfoliated and CVD samples on substrates is greater than one. For free standing graphene and wet exfoliated species always lower than one. Taking into account the previous considerations wet exfoliated material is closer to free standing graphene than the ones on substrates. The substrate may generate an extra damping for the G band phonons, which can lower the intensity of the G peak therefore changes the ratio.

3.2 Electron Spin Resonance spectroscopy ESR spectra of the investigated materials are presented in Fig. 2. All samples (including the SGN18 starting material) shows a narrow feature with a characteristic, uniaxial g-factor anisotropy lineshape, shown in the inset of Fig. 2. This signal most probably comes from defects which are embedded in the sp^2 matrix of graphene. This would explain the uniaxial nature of the g-factor anisotropy.

The broader component for the SGN18 graphite sample has a characteristic 12 mT ESR linewidth with a g-factor of 2.0148 [49,50]. The line originates from conducting electrons present in graphite, the value of g-factor is the weighted average of the two crystalline directions ($B \parallel c$ and $B \perp c$) with g-factors of the two, which are present in HOPG [51,52,49] with values of 2.0023 and 2.05. The broader component has a $1.1 - 1.4$ mT linewidth for the three FLG samples with a g-factor slightly above the free-electron value $g_0 = 2.0023$. We tentatively assign this signal to a few layer graphene phase which is p-doped due to the solvent molecules. p-doping by e.g. AsF_5 is known

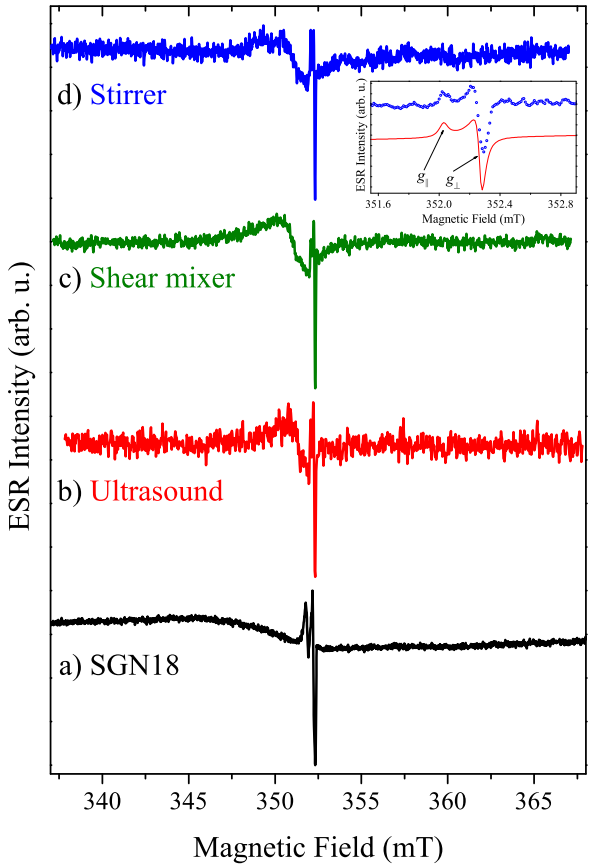

Figure 2 ESR spectra of a) SGN18 graphite powder, b) ultrasounded, c) shear mixed, d) stirred FLGs. The graphite powder has a broad line of about 12.2 mTs as expected at a g-factor of 2.0148. Ultrasounded FLG present a Lorentzian of 1.1 mT linewidth at $g = 2.0059$, the shear mixed present a 1.4 mT at $g = 2.0082$. The stirred material has a uniaxial anisotropic line with the width of 1.2 mT at $g = 2.0094$. The narrow uniaxial anisotropic line is coming from defects and dangling bonds in all cases. The inset shows the uniaxial g-factor simulated ESR lineshape for the narrow component in the stirrer prepared sample.

to give rise to similar signals with a $g > g_0$ [53]. Ultrasounded and shear mixed materials present a single derivative Lorentzian peak with a width of 1.1 mT and 1.4 mT, respectively. The stirred sample display a similar peak to graphite powder, but with a much narrower width of 1.2 mT. The g-factor of FLG materials is between the free electron and the graphite powders. The most probable explanation for this is that single layer sheets is giving a g-factor close to free electrons, but screened by the few layer sheets whose g-factor is closer to graphite. The sharp lines are associated with the defects and dangling bonds. In all materials the g-factor is below the free electrons 2.0023, thus can be associated with p-type charge carriers. The spectra were simulated with derivative Lorentzian lineshapes whose parameters are given in Table 3.2.

Table 3 g-factor, ΔB linewidth of the measured materials.

Broad component	SGN18	US	SM	ST
g	2.0148	2.0059	2.0082	2.0094
ΔB (mT)	12.2	1.1	1.4	1.2
Narrow component	SGN18	US	SM	ST
g	2.0014	2.0013	2.0006	2.0013
ΔB (mT)	0.08	0.04	0.04	0.04

Previous study done by Ciric [54] on mechanically exfoliated graphene showed a 0.62 mT wide peak with a g-factor of 2.0045. On reduced GO [55] a g-factor of 2.0062 and a width of 0.25 mT was found. The solvothermally synthesized graphene [56] shows a peak with a g-factor of 2.0044 and a width of 0.04 mT. According to these studies wet exfoliated graphene species have a g-factor close to reduced graphite, but with a width close to mechanically exfoliated and solvothermally synthesized.

3.3 Microwave resistance Microwave resistance of the investigated materials are presented in Fig. 3. This method is based on measuring the microwave loss due to the sample inside a microwave cavity. This contactless method is preferred when measuring resistance in powder samples, however the measured loss depends on the sample amount and morphology. It therefore provides accurate measurement of the *relative* temperature dependent resistance, however it does not allow for a direct measurement of the resistivity. The resistance is proportional to the inverse of the microwave loss and it is normalized to that of SGN18 at 25 K to get comparable results. Microscope images are presented as insets of Fig. 3. to demonstrate the difference in grain size.

All the measured materials have a semi-conducting behavior in the investigated temperature range. This behavior is usual to defective and inhomogeneous polycrystalline metals. The difference in the microwave loss in the different samples is primarily due to a difference in the grain size. The loss, L, is know to scale with the average grain size as $L = \pi B_0^2 \sigma R^5/5$, where B_0 is the amplitude of the magnetic field, σ is the conductivity, and R is the average radius of the grains [44,57]. The average grain size was obtained as about $3-5$ millimeters, 500 μm, and 300 microns for the ultrasounded, stirred and shear mixed samples, respectively, by analyzing the corresponding microscope images. The trend in the microwave loss between the different samples is thus found to follow the grain size.

4 Conclusions We studied the vibrational, magnetic and transport properties of mechanically different post processed few layer graphene systems with Raman, ESR spectroscopy and microwave resistance measurements respectively. According to the results the difference in post procession does effect the investigated properties. From our results one can figure out that ultrasound treatment ends up with the best results in a meaning that this is the closest to true single layer graphene.

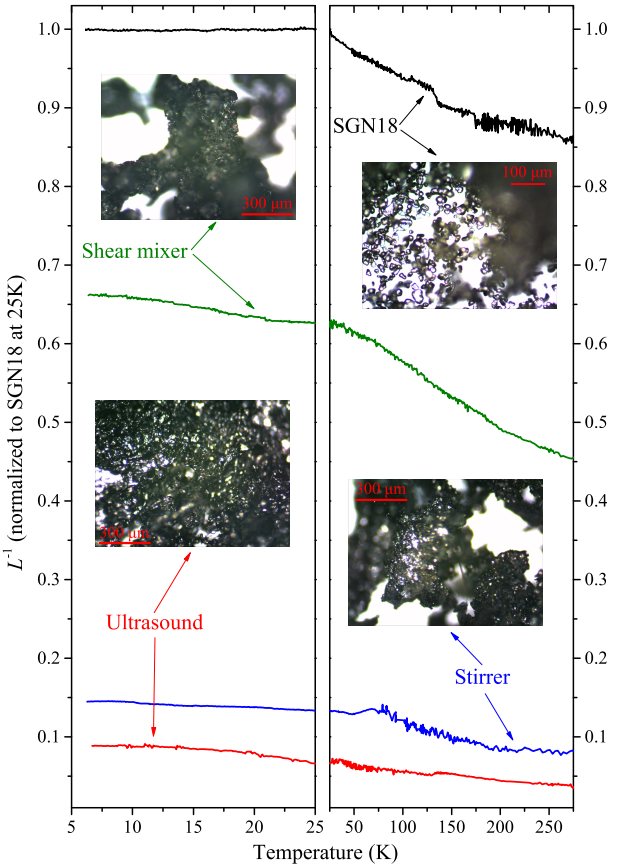

Figure 3 Microwave resistance of FLGs compared to graphite. Insets are microscope images from the materials. Note the different scale for the SGN18 graphite sample. The different resistance of FLG species can be explained with the different grain size.

Acknowledgements Work supported by the European Research Council Grant No. ERC-259374-Sylo.

References

[1] H. W. Kroto, J. R. Heath, S. C. O'Brien, R. F. Curl, and R. E. Smalley, Nature **318**, 162 – 163 (1985).
[2] S. Iijima, Nature **354**, 56 – 58 (1991).
[3] K. S. Novoselov, A. K. Geim, S. V. Morozov, D. Jiang, Y. Zhang, S. V. Dubonos, I. V. Grigorieva, and A. A. Firsov, Science **306**, 666–669 (2004).
[4] A. K. Geim and K. S. Novoselov, Nature Materials **6**, 183 – 191 (2007).
[5] A. K. Geim, Science **324**, 1530–1534 (2009).
[6] A. H. C. Neto, F. Guinea, N. M. R. Peres, K. S. Novoselov, and A. K. Geim, Reviews of Modern Physics **81**, 109–162 (2009).
[7] B. Jayasena and S. Subbiah, Nanoscale Research Letters **6**(1), 95 (2011).
[8] C. Berger, Z. Song, X. Li, X. Wu, N. Brown, C. Naud, D. Mayou, T. Li, J. Hass, A. N. Marchenkov, E. H. Conrad, P. N. First, and W. A. de Heer, Science **312**, 1191–1196 (2006).
[9] S. Y. Zhou, G. H. Gweon, A. V. Fedorov, P. N. First, W. A. de Heer, D. H. Lee, F. Guinea, A. H. C. Neto, and A. Lanzara, Nature Materials **6**, 770 – 775 (2007).
[10] P. W. Sutter, J. I. Flege, and E. A. Sutter, Nature Materials **7**, 406 – 411 (2008).
[11] A. N. Obraztsov, E. A. Obraztsova, A. V. Tyurnina, and A. A. Zolotukhin, Carbon **45**, 2017–2021 (2007).
[12] A. Malesevic, R. Vitchev, K. Schouteden, A. Volodin, L. Zhang, G. V. Tendeloo, A. Vanhulsel, and C. V. Haesendonck, Nanotechnology **19**, 305604 (2008).
[13] K. S. Kim, Y. Zhao, H. Jang, S. Y. Lee, J. M. Kim, K. S. Kim, J. H. Ahn, P. Kim, J. Y. Choi, and B. H. Hong, Nature Letters **457**, 706–710 (2009).
[14] A. N. Obraztsov, Nature Nanotechnology **4**, 212–213 (2009).
[15] A. Reina, X. Jia, J. Ho, D. Nezich, H. Son, V. Bulovic, M. S. Dresselhaus, and J. Kong, Nano Letters **9**(1), 30–35 (2009).
[16] C. Mattevi, H. Kima, and M. Chhowalla, Journal of Materials Chemistry **21**, 3324–3334 (2011).
[17] Q. Yu, L. A. Jauregui, W. Wu, R. Colby, J. Tian, Z. Su, H. Cao, Z. Liu, D. Pandey, D. Wei, T. F. Chung, P. Peng, N. P. Guisinger, E. A. Stach, J. Bao, S. S. Pei, and Y. P. Chen, Nature Materials **10**, 443–449 (2011).
[18] C. C. Chen, W. Bao, J. Theiss, C. Dames, C. N. Lau, and S. B. Cronin, Nano Letters **9**(12), 4172–4176 (2009).
[19] A. C. Ferrari, J. C. Meyer, V. Scardaci, C. Casiraghi, M. Lazzeri, F. Mauri, S. Piscanec, D. Jiang, K. S. Novoselov, S. Roth, and A. K. Geim, Physical Review Letters **97**, 187401 (2006).
[20] A. Das, B. Chakraborty, and A. K. Sood, Bull. Mater. Sci. **31**(3), 579–584 (2008).
[21] C. Faugeras, A. Nerriere, and M. Potemski, Applied Physics Letters **92**, 011914 (2008).
[22] J. Tsurumi, Y. Saito, and P. Verma, Chemical Physics Letters **557**, 114–117 (2013).
[23] C. Gomez-Navarro, R. T. Weitz, A. M. Bittner, M. Scolari, A. Mews, M. Burghard, and K. Kern, Nano Letters **7**(11), 3499–3503 (2007).
[24] Z. Osváth, A. Darabont, P. Nemes-Incze, E. Horváth, Z. E. Horváth, and L. P. Biró, Carbon **45**, 3022–3026 (2007).
[25] S. Stankovich, D. A. Dikin, R. D. Piner, K. A. Kohlhaas, A. Kleinhammes, Y. Jia, Y. Wu, S. T. Nguyen, and R. S. Ruoff, Carbon **45**, 1558–1565 (2007).
[26] G. Eda, G. Fanchini, and M. Chhowalla, Nature Letters **3**, 270–274 (2008).
[27] S. Park and R. S. Ruoff, Nature Nanotechnology **4**, 217–224 (2009).
[28] D. R. Dreyer, S. Park, C. W. Bielawski, and R. S. Ruoff, Chemical Society Reviews **39**, 228–240 (2010).
[29] Y. Shao, J. Wang, M. Engelhard, C. Wang, and Y. Lin, Journal of Materials Chemistry **20**, 743–748 (2010).
[30] J. Zhang, H. Yang, G. Shen, P. Cheng, J. Zhang, and S. Guo, Chem. Commun. **46**, 1112–1114 (2010).
[31] W. Chen, L. Yan, and P. R. Bangal, Carbon **48**, 1146–1152 (2010).
[32] W. Chen, L. Yan, and P. R. Bangal, J. Phys. Chem **114**, 19885–19890 (2010).
[33] S. Pei, J. Zhao, J. Du, W. Ren, and H. M. Cheng, Carbon **48**, 4466 –4474 (2010).

[34] E. C. Salas, Z. Sun, A. Lüttge, and J. M. Tour, Carbon **48**, 4466 –4474 (2010).
[35] S. Pei and H. M. Cheng, Carbon **50**, 3210 –3228 (2012).
[36] Y. Hernandez, V. Nicolosi, M. Lotya, F. M. Blighe, Z. Sun, S. De, I. T. McGovern, B. Holland, M. Byrne, Y. K. Gun'ko, J. J. Boland, P. Niraj, G. Duesberg, S. Krishnamurthy, R. Goodhue, J. Hutchison, V. Scardaci, A. C. Ferrari, and J. N. Coleman, Nature Nanotechnology **3**, 563–568 (2008).
[37] J. M. Englert, J. Roöhrl, C. D. Schmidt, R. Graupner, M. Hundhausen, F. Hauke, and A. Hirsch, Adv. Mater. **21**, 4265–4269 (2009).
[38] M. Lotya, Y. Hernandez, P. J. King, R. J. Smith, V. Nicolosi, . S. Karlsson, F. M. Blighe, S. De, Z. Wang, I. T. McGovern, G. S. Duesberg, and J. N. Coleman, J. Am. Chem. Soc. **131**, 3611–3620 (2009).
[39] J. M. Englert, C. Dotzer, G. Yang, M. Schmid, C. Papp, J. M. Gottfried, H. P. Steinrück, E. Spiecker, F. Hauke, and A. Hirsch, Nature Chemistry **3**, 279–286 (2011).
[40] J. Coleman, Accounts of Chemical Research (2013).
[41] A. Hirsch, J. M. Englert, and F. Hauke, Accounts of Chemical Research **1**, 87–96 (2013).
[42] P. Vecera, J. C. Chacón-Torres, S. Reich, F. Hauke, and A. Hirsch, handout (2015).
[43] G. Fábián, C. Kramberger, A. Friedrich, F. Simon, and T. Pichler, Review of Scientific Instruments **82**, 023905 (2011).
[44] O. Klein, S. Donovan, M. Dressel, and G. Grüner, International Journal of Infrared and Millimeter Waves **14**(12), 2423–2456 (1993).
[45] S. Donovan, O. Klein, M. Dressel, K. Holczer, and G. Grüner, International Journal of Infrared and Millimeter Waves **14**(12), 2459–2487 (1993).
[46] B. Nebendahl, D. N. Peligrad, M. Pozek, A. Dulcic, and M. Mehring, Review of Scientific Instruments **72**, 1876–1881 (2001).
[47] Y. Wang, D. C. Alsmeyer, and R. L. McCreery, Chem. Mater. **2**, 557–563 (1990).
[48] Z. H. Ni, T. Yu, Z. Q. Luo, Y. Y. Wang, L. Liu, C. P. Wong, J. Miao, W. Huang, and Z. X. Shen, ACS Nano **3**(3), 569 – 574 (2009).
[49] D. L. Huber, R. R. Urbano, M. S. Sercheli, and C. Rettori, Phys. Rev. B **70**, 125417 (2004).
[50] M. Galambos, G. Fábián, F. Simon, L. Ćirić, L. Forró, L. Korecz, A. Rockenbauer, J. Koltai, V. Zólyomi, A. Rusznyák, J. Kürti, N. M. Nemes, B. Dóra, H. Peterlik, R. Pfeiffer, H. Kuzmany, and T. Pichler, Phys. Status Solidi B **246**(11–12), 2760–2763 (2009).
[51] M. Sercheli, Y. Kopelevich, R. R. da Silva, J. H. S. Torres, and C. Rettori, Physica B **320**, 413–415 (2002).
[52] M. Sercheli, Y. Kopelevich, R. R. da Silva, J. H. S. Torres, and C. Rettori, Solid State Communications **121**, 579–583 (2002).
[53] M. S. Dresselhaus and G. Dresselhaus, Advances in Physics **30**, 1–186 (1981).
[54] L. Ćirić, A. Sienkiewicz, B. Náfrádi, M. Mionić, A. Magrez, and L. Forró, Phys. Status Solidi B **246**(11–12), 2558–2561 (2009).
[55] L. Ćirić, A. Sienkiewicz, R. Gaál, J. Jaćimović, C. Vâju, A. Magrez, and L. Forró, Phys. Rev. B **86**, 195139 (2012).
[56] B. Náfrádi, M. Choucair, and L. Forró, Carbon **74**, 346–351 (2014).
[57] H. Kitano, R. Matsuo, K. Miwa, A. Maeda, T. Takenobu, Y. Iwasa, and T. Mitani, Phys. Rev. Letters **88**(9), 096401 (2002).